

# Impurity behaviors of nitrogen in W–C–N thin diffusion barriers for Cu metallization schemes

Soo In Kim · Chang Woo Lee

Received: 28 May 2007 / Accepted: 8 April 2008 / Published online: 8 May 2008  
© Springer Science + Business Media, LLC 2008

**Abstract** To investigate the effect of nitrogen impurities in the tungsten–carbon thin films, the electrical and structural properties of W–C–N thin films deposited with rf magnetron sputtering method were measured. Interface characteristics of W–C–N/Si were studied with resistivity and crystal structure as a function of nitrogen impurity concentrations of as-deposited and annealed state for various annealing temperature. We also investigate the interface of Cu/W–C–N/Si for various nitrogen concentration by using XRD pattern and Nomarski microscope. Our experimental results indicate that nitrogen impurity provides stuffing effect for preventing the interdiffusion between Cu and Si interface after annealing up to 800°C for 30 min, because W–C–N thin films serve as a good diffusion barrier and this may be due to the role of nitrogen and carbon inside the W–C–N film not as bonded state but impurities

**Keywords** W–C–N thin film · Diffusion barrier · Copper metallization

## 1 Introduction

The geometrical dimensions of ultra large-scale integrated (ULSI) devices continue to shrink. Also, submicron process needs multi layer and film thickness needs to be shallow. Thus, the size of multilevel interconnects of ULSI devices is critical, and it is necessary both to reduce the RC time delay for device speed performance and to get higher densities without electromigration [1, 2]. From this reason,

at the semiconductor production technology, wiring progress is used Cu metals. But these metal–nitride barriers have many problems, such as poor step coverage, residual stress, and poor control of stoichiometry of the metal–nitride composition. Moreover, the interaction between Cu and Si is strong and detrimental to the electrical performance of Si even at temperatures below 400°C [3]. Therefore, it is necessary to implement a barrier layer between Si and Cu [4–7]. In this research, we suggest the tungsten–carbon–nitrogen thin film as a stuffing diffusion barrier for preventing the Cu diffusion through Si substrate. Recently, we reported W–N and W–B–N thin films prepared by using a plasma-enhanced chemical vapor deposition (PECVD) method and rf magnetron sputtering method, which are very effective for preventing the silicidation and encroachment. This report using rf magnetron sputtering (PVD method). PVD method is very simple and valuable. From this reason, W–C–N diffusion barrier have advantage over any other diffusion barrier. From this study, we get the nitrogen impurity effects of W–C–N thin films by stuffing effect that was very effective for preventing the interdiffusion between metal and silicon during subsequent high-temperature annealing process. In order to improve the characteristics of diffusion barrier, we examined the impurity behaviors for various nitrogen concentration.

## 2 Experiments

Tungsten carbon nitride thin films were deposited on Si substrates by using a magnetron sputtering system. Substrates were p-doped (100) oriented Si wafers with resistivities of  $5 \times 6 \Omega \text{ cm}$ . Prior to sputtering, substrates were cleaned (by using RCA method), spun-dried, and loaded into deposition chamber. Sputtering targets were tungsten (W) with a purity

---

S. I. Kim · C. W. Lee (✉)  
Nano & Electronic Physics, Kookmin University,  
Seoul 136-702, Korea  
e-mail: cwlee@kookmin.ac.kr

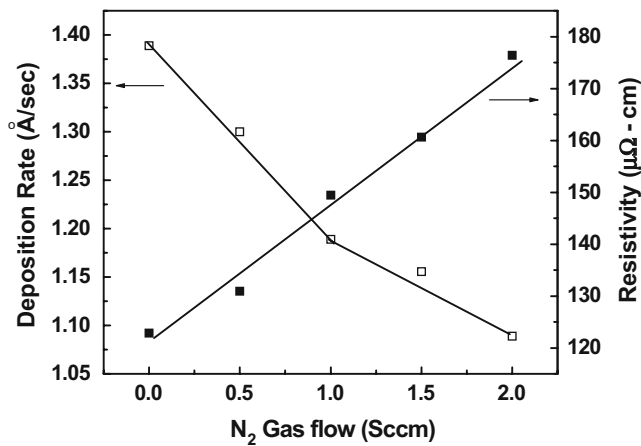


**Fig. 1** The resistivity and the deposition rate vs N<sub>2</sub> gas flow of W–C–N thin films for as-deposited states

of 99.99%, and tungsten carbide (WC) with a purity of 99.95%. Before deposition, Ar pre-sputtering was performed to remove native oxide layer on top of target. Deposition temperature was maintained at room temperature during sputtering process. The flow rates of N<sub>2</sub> and Ar gases were separately controlled with mass flow controllers. The total pressure of sputtering reactor was kept at a constant value of 3 mTorr while N<sub>2</sub> gas flow (sccm) was varied from 0 to 2 sccm. The co-sputtering condition was that the RF power density of W target and WC target power were fixed. W and WC target had 2 in. diameter and 1/4 in. thickness. The thickness of W–C–N thin film was varied from 50 to 100 nm.

The resistances and the crystalline structures of as-deposited W–C–N thin films were determined with a four-point probe and X-ray diffraction (XRD), respectively. Annealing process was performed from as-deposited to 1000°C for 30 min in a N<sub>2</sub> ambient. Copper was coated on the W–C–N/Si substrate by using a thermal evaporator.

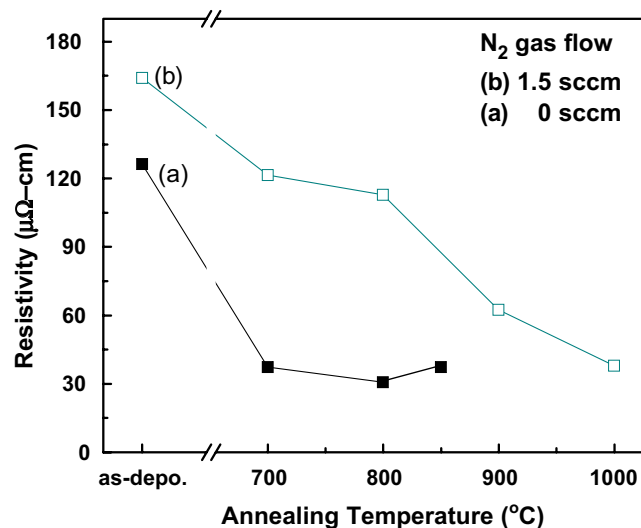


**Fig. 2** The resistivity of W–C–N thin films as a function of annealing temperature for N<sub>2</sub> gas flow of (a) 0 sccm and (b) 1.5 sccm

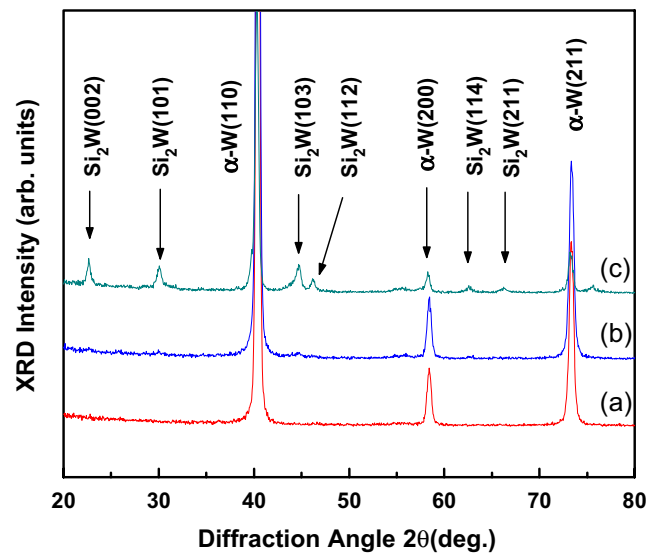


**Fig. 3** The XRD patterns of W–C–N thin films as a N<sub>2</sub> gas flow of 0 sccm after annealing at (a) 700°C, (b) 800°C, and (c) 850°C for 30 min, respectively

Annealing process was performed from 650°C to 850°C for 30 min in a N<sub>2</sub> ambient. The phase transformation of W–C–N thin film and the interfacial reactions of Cu/W–C–N thin films annealed at various temperatures were investigated by using XRD. The surface characteristics were studied by Nomarski microscope.

### 3 Results and discussion

Figure 1 shows the deposition rate and the resistivity as a function of N<sub>2</sub> gas flow (sccm) of W–C–N thin films for as-

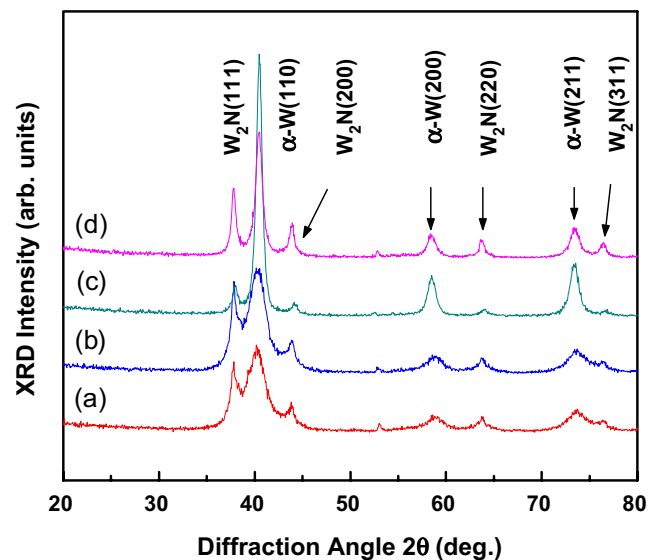


**Fig. 4** The XRD patterns of W–C–N thin films as a N<sub>2</sub> gas flow of 1.5 sccm after annealing at (a) 700°C, (b) 800°C, (c) 900°C, and (d) 1000°C for 30 min, respectively

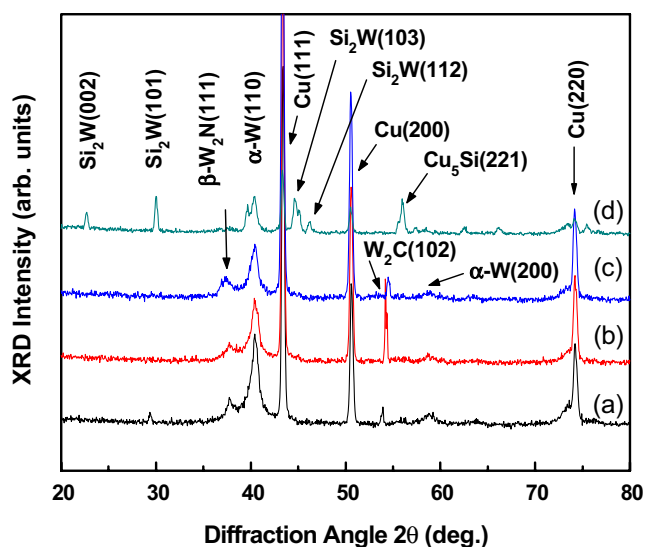


**Fig. 5** The XRD patterns of Cu/W–C–N thin films as a  $N_2$  gas flow of 1.5 sccm after annealing at (a) 650°C, (b) 700°C, (c) 750°C, and (d) 850°C for 30 min, respectively

deposited and annealed states. The deposition rate decreased from 1.34 to 1.19 Å/s as the  $N_2$  gas flow rate was changed from 0 to 1 sccm. Also the deposition rate decreased slowly from 1.19 to 1.09 Å/s as the  $N_2$  gas flow changed from 1 to 2 sccm. The resistivity increased from 123.8 to 176.4  $\mu\Omega$  cm as  $N_2$  gas flow increased linearly from 0 to 2 sccm.

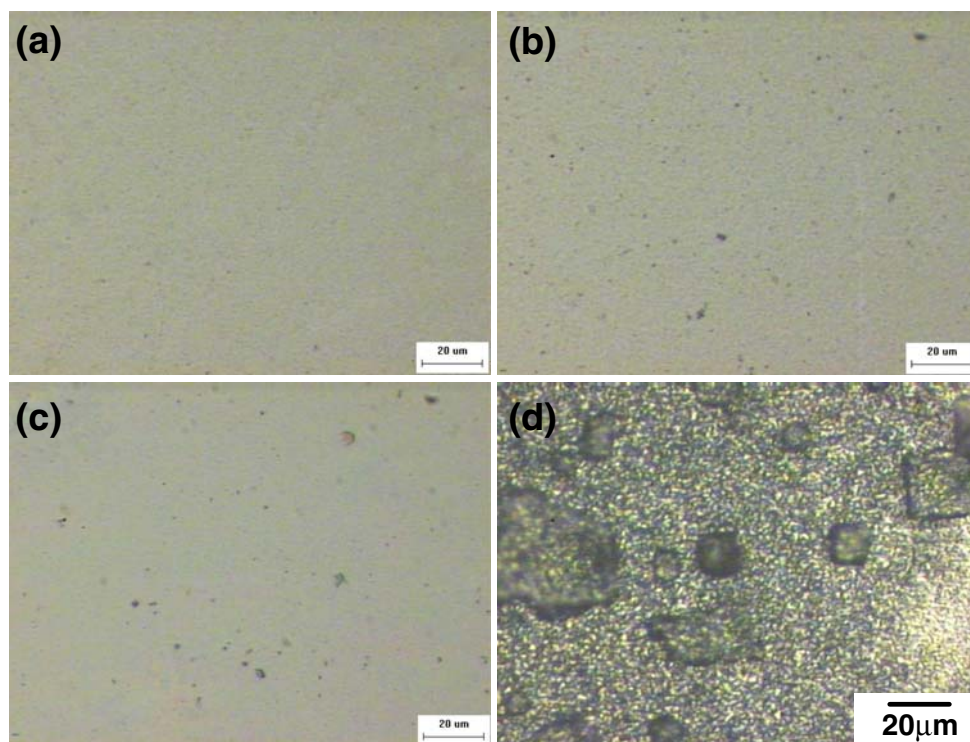
Figure 2 shows the resistivity of W–C–N thin films as a function of annealing temperature for  $N_2$  gas flow from 0 to

1.5 sccm. For the  $N_2$  gas flow of 0 sccm, the resistivity decreased from 122.85  $\mu\Omega$  cm to 33.74  $\mu\Omega$  cm as annealing temperature decreased rapidly from as-deposited state to 700°C. The resistivity was a little bit increased as annealing temperature increased from 800 to 850°C. W–C thin films did form silicide peaks on Si after annealing temperatures up to 850°C. However,  $N_2$  gas flow of 1.5 sccm, the resistivity decreased from 160.67  $\mu\Omega$  cm to 34.45  $\mu\Omega$  cm as annealing temperature increased from as-deposited state to 1000°C. The W–C–N thin films did not form any silicide peak on Si after annealing temperatures up to 1000°C. From these results, the role of nitrogen inside the W–C–N thin films was not bonded state but impurities. So we measured XRD diffraction at  $N_2$  gas flow of 0 and 1.5 sccm.

Figure 3 shows the XRD patterns of W–C thin films for the  $N_2$  gas flow of 0 sccm after annealing from 700°C to 850°C for 30 min, respectively. Fig. 3(a) and (b) show that (110), (200) and (211) oriented  $\alpha$ -W peaks were apparent at 40.40°, 58.37° and 73.23°, respectively. Fig. 3(c) shows that (110), (200) and (211) oriented  $\alpha$ -W peaks were occurred at 40.32°, 58.34° and 73.17° along with (002), (101), (103), (112), (114), and (211) oriented  $Si_2W$  peaks occurring at 22.67°, 30.14°, 44.77°, 46.22°, 62.63°, and 66.25°, respectively. Thus, the W–C thin films did protect the interdiffusion between metal and Si after annealing temperatures up to 800°C.

Figure 4 shows the XRD patterns of W–C–N thin films at the  $N_2$  gas flow of 1.5 sccm after annealing from 700°C to 1000°C for 30 min, respectively. Fig. 4 shows that the

**Fig. 6** Nomarski micrographs of Si surface for Cu/W–C–N/Si thin film produced as a  $N_2$  gas flow of 1.5 sccm for various annealing temperatures of (a) 650°C, (b) 700°C, (c) 750°C and (d) 850°C



(111), (200), (220) and (311) oriented  $W_2N$  peaks were observed at  $37.73^\circ$ ,  $43.87^\circ$ ,  $63.78^\circ$ , and  $76.58^\circ$  along with (110), (200), and (211) oriented  $\alpha$ -W peaks were occurred at  $40.34^\circ$ ,  $58.44^\circ$  and  $73.25^\circ$ , respectively. Fig. 4 indicates the formation of  $N_2$  constituent in W–C–N thin films. From these XRD results, the role of nitrogen impurity of W–C–N thin films was stuffing effect that the W–C–N thin film was very effective for preventing the interdiffusion between metal and silicon during the subsequent high-temperature annealing process. That is, W–C thin films (not included  $N_2$  concentration) was protected up to  $800^\circ C$  but W–C–N thin films (included  $N_2$  constituent) was protected up to  $1000^\circ C$  from Figs. 3 and 4.

We also investigated the role of an interface layer, such as a W–C–N layer, between Cu metal and Si substrate. The Cu/W–C–N/Si thin films were annealed at various annealing temperatures.

Figure 5 shows the XRD patterns of Cu/W–C–N thin films with the  $N_2$  gas flow of 1.5 sccm after annealing from  $650^\circ C$  to  $850^\circ C$  for 30 min, respectively. Fig. 5 shows that (111), (200) and (220) oriented Cu peaks were appeared at  $43.40^\circ$ ,  $50.56^\circ$  and  $74.13^\circ$  and (110) oriented  $\alpha$ -W peak was occurred at  $40.51^\circ$ , along with (111) oriented  $\beta$ - $W_2N$  peak was occurred at  $37.21^\circ$ , respectively. Fig. 5(d) shows that (111), (200), and (220) oriented Cu peaks were occurred at  $43.33^\circ$ ,  $50.50^\circ$  and  $74.15^\circ$ , along with (110) oriented  $\alpha$ -W peak was occurred at  $40.39^\circ$ , (002), (101), (103), and (112) oriented  $Si_2W$  peaks at  $22.67^\circ$ ,  $29.99^\circ$ ,  $44.60^\circ$ , and  $46.23^\circ$ , (221) oriented  $Cu_5Si$  peak at  $57.36^\circ$  after annealing at  $800^\circ C$ , respectively. From these results, we confirm that no other copper silicides were formed during annealing up to  $750^\circ C$ . This may be due to the role of carbon and nitrogen inside the W–C–N film not as a bonded state but impurities.

After that, Cu and W–C–N thin film were preferentially etched with a Wright etchant, which was useful for observation of defects generated by the interdiffusion of Cu and Si. Figure 6 shows the Nomarski micrographs of the Si surface after the Cu and W–C–N thin film had been

annealed for various annealing temperatures for 30 min and etched. In the W–C–N thin film deposited at a  $N_2$  gas flow of 1.5 sccm, neither Cu-decorated microdefects nor dislocations appeared after annealing even at  $750^\circ C$ . However, Cu-decorated defects was observed after annealing at  $850^\circ C$ . Cu atoms had penetrated through the W–C–N diffusion barrier, and it had diffused into the Si substrate along (110) direction that had generated many dislocations.

#### 4 Conclusion

In this work, tungsten–carbon–nitride (W–C–N) diffusion barrier were examined to prevent the interdiffusion between Cu and Si substrate as well as the effect of  $N_2$  concentration. W–C–N thin films on Si substrate had good thermal stability up to  $1000^\circ C$  at the  $N_2$  gas flow of 1.5 sccm. Also Cu did not diffuse through the W–C–N thin films after being annealed at  $750^\circ C$  for 30 min. Here, the W–C–N thin films at a  $N_2$  gas flow of 1.5 sccm were very effective for preventing Cu diffusion since Cu-decorated defects were not formed after annealing at  $750^\circ C$ .

**Acknowledgment** This work was financially supported by research program 2007 of Kookmin University in Korea.

#### References

1. H. Park, S.J. Hwang, Y.C. Joo, *Acta Mat.* **52**(8), 2435 (2004)
2. C.W. Lee, J.G. Kim, *Phys. Stat. Sol. (B)*. **241**(7), 1645 (2004)
3. C. Weaver, *J. Vac. Sci. Technol.* **12**, 18 (1975)
4. C.W. Lee, Y.T. Kim, *J. Vac. Sci. Technol. B*. **24**(6), 1432 (2006). DOI [10.1116/1.2203639](https://doi.org/10.1116/1.2203639)
5. Y.T. Kim, C.W. Lee, S.K. Min, *Jpn. J. Appl. Phys.* **32**, 6126 (1993). DOI [10.1143/JJAP.32.6126](https://doi.org/10.1143/JJAP.32.6126)
6. Y.T. Kim, C.W. Lee, C.W. Han, S.K. Min, *Appl. Phys. Lett.* **61**, 1205 (1992). DOI [10.1063/1.107595](https://doi.org/10.1063/1.107595)
7. B.H. Lee, K.S. Lee, D.K. Shon, J.S. Byun, *Appl. Phys. Lett.* **76** (18), 2538 (2000). DOI [10.1063/1.126401](https://doi.org/10.1063/1.126401)